Imerito, R. Merom, R. Olthof-Hazenkamp, M. A. Spackman, N. Spadaccini and J. M. Stewart to the *XTAL*3.0 system (Hall & Stewart, 1990), used extensively in this work, is gratefully acknowledged. Thanks are also due to D. C. Creagh for evaluating the dispersion corrections to the atomic scattering factors. The authors also acknowledge the support of the Austalian Research Council, and of the Japanese Ministry of Education.

References

ALCOCK, N. W. (1974). *Acta Cryst.* A**30**, 332–335.
BACHMAN, R., KOHLER, H., SCHULZ, H. & WEBER, H.-P. (1985). *Acta Cryst.* A**41**, 35–40.
BUTTNER, R. H. & MALSEN, E. N. (1988). *Acta Cryst.* C**44**, 1707–1709.
CREAGH, D. C. (1990). Private communication.
HALL, S. R. & STEWART, J. M. (1990). Editors. *XTAL*3.0 *User's Manual*. Univs. of Western Australia, Australia, and Maryland, USA.
HIRSHFELD, F. L. (1977). *Isr. J. Chem.* **16**, 198–201.
MASLEN, E. N. (1990). Private communication.
MASLEN, E. N. & SPADACCINI, N. (1989). *Acta Cryst.* B**45**, 45–52.
MASLEN, E. N. & SPADACCINI, N. (1993). *Acta Cryst.* A**49**. In the press.
REES, B. (1977). *Isr. J. Chem.* **16**, 180–186.
SATOW, Y. & IITAKA, Y. (1989). *Rev. Sci. Instrum.* **60**, 2390–2393.

Acta Cryst. (1993). B**49**, 636–641

X-ray Study of the Electron Density in Calcite, $CaCO_3$

BY E. N. MASLEN, V. A. STRELTSOV AND N. R. STRELTSOVA

Crystallography Centre, University of Western Australia, Nedlands, Western Australia 6009, *Australia*

(*Received* 17 *November* 1992; *accepted* 10 *March* 1993)

Abstract

The electron density in synthetic calcite, $CaCO_3$, has been determined using diffraction data for a naturally faced single crystal measured with X-ray Mo $K\alpha$ ($\lambda = 0.71073$ Å) radiation. Extinction corrections that minimize differences between equivalent reflection intensities are closely approximated by the values which optimize the extinction parameter as part of the least-squares structure refinement. Deformation electron densities evaluated with the two techniques are closely similar. There are 0.26 e Å^{-3} high-density maxima in the C—O bonds and 0.28 e Å^{-3} maxima at the O-atom lone pairs. There is no evidence in the least-squares parameters and deformation maps for deviation from CO_3-group planarity or disorder. Space group $R\bar{3}c$, hexagonal, $M_r = 100.09$, $a = 4.991$ (2), $c = 17.062$ (2) Å, $V = 368.1$ (3) Å^3, $Z = 6$, $D_x = 2.709$ Mg m^{-3}, μ(Mo $K\alpha$) $= 2.134$ mm^{-1}, $F(000) = 300$, $T = 293$ K, $R = 0.017$, $wR = 0.023$, $S = 4.52$ for 328 unique reflections.

Introduction

Calcite, $CaCO_3$, is an abundant carbonate mineral. Its structure is isomorphous with that of several carbonate constituents of sedimentary rocks, including magnesium- and iron-bearing carbonates. These calcite-type minerals are often used as model compounds for investigating structural sources of optical anisotropy.

The calcite structure has the same space group, $R\bar{3}c$, as another widely distributed mineral, corundum (α-Al_2O_3), for which the electron density has been measured several times over the past decade. Deformation-density maps in a recent synchrotron radiation study of a small corundum specimen by Maslen, Streltsov, Streltsova, Ishizawa & Satow (1993) differ significantly from those reported previously. The discrepancies were attributed to the extinction corrections which in the earlier studies were determined by refining the corrections along with the structure by least-squares minimizing of differences between observed and calculated structure factors (Streltsov & Maslen, 1992).

In an alternative approach to extinction corrections for small crystals, Maslen & Spadaccini (1993) determine extinction parameters by least-squares minimizing of differences between intensities for equivalent reflections with different path lengths. This eliminates any dependence of the extinction estimates on structure-factor models which may occur if corrections are determined as part of the structure refinement. The number of equivalent reflection intensities for high-symmetry structures is larger than the number of observations relevant to extinction in structure refinements with symmetry-unique observations. This increase in numbers improves the statistical significance of the results which are derived. For corundum the influence of extinction on the diffraction data indicated by the equivalent-reflection technique was much smaller

than that indicated by the structure refinement. It is therefore desirable to compare the extinction-correction behaviour determined for corundum with that for the closely related calcite structure.

The one communication on the electron density in calcite itself (Peterson, Ross, Gibbs, Chiari, Gupta & Tossell, 1979) is short and preliminary, in contrast with extensive studies of the electron density in the mineral magnesite, $MgCO_3$, by Göttlicher & Vegas (1988), and in the mineral dolomite, $CaMg(CO_3)_2$, by Effenberger, Kirfel & Will (1983). The nature of *Me*—O bonds was the focal point of interest in both those studies. Göttlicher & Vegas (1988) explained the electron-density map for magnesite in terms of ionic interactions between Mg and CO_3 ions, but Effenberger, Kirfel & Will (1983) interpreted positive regions in the deformation-density maps at the midpoints of the Ca—O and Mg—O for dolomite in terms of covalency in those bonds. If both conclusions were correct, one should expect calcite to show a higher degree of covalency, characterized by increased positive density at the midpoint of the *Me*—O bond.

Göttlicher & Vegas (1988) observed an electron-density bridge between O atoms along the longest edge of the MgO_6 octahedron in magnesite. That contrasts with lower density near a short O—O distance outside the coordinate MeO_6 octahedron (*e.g.* the O—O2 distance in Fig. 1), which for magnesite is the shortest non-bonding O—O contact among all calcite-type carbonates. The corresponding contact in calcite is the largest among the rhombohedral carbonates (Effenberger, Mereiter & Zemann, 1981). Thus magnesite and calcite span the extreme range of lengths for this contact in this series of isomorphous structures.

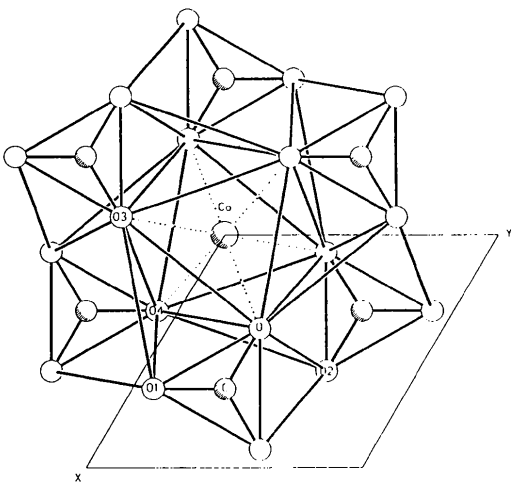

Fig. 1. Projection down the hexagonal *c* axis of a portion of the calcite structure showing the central Ca atom coordinated to six O atoms from distinct CO_3 groups.

A pyramidal distortion of the CO_3 group in dolomite with the C atom shifted by 0.018 (1) Å from the CO_3 plane was reported by Effenberger, Kirfel & Will (1983). Several authors have suggested that the CO_3 group in calcite is disordered. However rigid-body analysis of the CO_3-group vibrations, considered by others to be consistent with positional disorder, was interpreted by Peterson, Ross, Gibbs, Chiari, Gupta & Tossell (1979) as indicating screw motion of the CO_3 group parallel to the hexagonal *c* crystal axis. No disorder in the planar CO_3 anion was observed by Göttlicher & Vegas (1988) in magnesite.

Experimental

$CaCO_3$ crystals with natural faces were grown from aqueous solution by slow diffusion. Freshly prepared 0.2 *M* $Ca(NO_3)_2$ and 0.25 *M* Na_2CO_3 solutions, inserted at opposite ends of a W-shaped polycarbonate tube, were separated by several drops of water. After approximately two weeks the tube was cut open and the transparent colourless $CaCO_3$ crystals were removed for examination. A specimen selected for the X-ray diffraction measurements was bounded by two {104}, two {$\bar{1}$14}, two {0$\bar{1}$4} and one {1$\bar{2}$3} faces with dimensions 31 × 36 × 46 × 37 μm from the crystal centre, respectively. These dimensions were measured and the faces indexed using optical and scanning electron Philips SEM505 microscopes.

Diffraction data were measured on a Syntex *P*3 four-circle diffractometer. Mo *Kα* radiation (λ = 0.71073 Å) from an X-ray tube was monochromated with an oriented graphite monochromator in the equatorial setting. Lattice constants were determined from 30 reflections with 2θ values $40 < 2\theta < 50°$. Reflection intensities were measured systematically for a complete sphere of reciprocal space with $(\sin\theta/\lambda)_{max} = 1.08$ Å^{-1} using $\theta/2\theta$ scans $-10 \le h \le 10$, $-10 \le k \le 10$, $-36 \le l \le 36$. Six standard reflections were monitored every 100 reflections to check the stability of the incident beam. Integrated intensities for all the accessible reflections were calculated using the profile analysis program of Streltsov & Zavodnik (1989). The measured intensities were modified for fluctuation of the standards by Rees (1977). The variances in measured structure factors from counting statistics were modified for source instability as indicated by the standards and increased when necessary by comparing intensities of equivalent reflections following a Fisher test. Reflections having measured variances consistent with Poisson statistics were assigned the Poisson variance. Variances for other reflections were adjusted according to the scatter of equivalents.

The linear absorption coefficient μ at Mo $K\alpha$ was evaluated from atomic absorption coefficients by Creagh (1992). Lorentz–polarization corrections were applied and absorption corrections (Alcock, 1974) evaluated analytically. Corrections for thermal diffuse scattering (TDS), estimated with the program *TDS2* (Stevens, 1974) using elastic constants for calcite from *Landoldt-Börnstein* (Hellwege, 1966), were negligible. Extinction corrections were determined for the full data sets by the method of Maslen & Spadaccini (1993) before structural parameters were refined. All calculations utilized the *XTAL*3.2 system of crystallographic programs (Hall, Flack & Stewart, 1992) implemented on DEC 5000/120 workstation computers. Further experimental and refinement details are given in Table 1.

The reference state for structure-factor calculations was the independent atom model (IAM), using structure factors evaluated with spherical atomic scattering factors from *International Tables for X-ray Crystallography* (1974, Vol. IV), and dispersion corrections $\Delta f'$, $\Delta f''$ of 0.227, 0.308 for Ca, and 0.007, 0.002 for C, and 0.012, 0.006 for O at Mo $K\alpha$ evaluated by Creagh (1992). Ten independent parameters, including the anisotropic vibration tensor elements, were determined by full-matrix least-squares refinement based on $|F|$ with least-squares weights equal to $1/\sigma^2(F_o)$ for all measured structure factors. Details are given in Tables 1 and 2.† An isotropic extinction parameter r^* (Larson, 1970) was evaluated during structure refinement for comparison with that from the method of Maslen & Spadaccini (1993). The very close agreement for the two results listed in Table 1 is in marked contrast with the corresponding extinction estimates for α-Al_2O_3 (Streltsov & Maslen, 1992; Maslen, Streltsov, Streltsova, Ishizawa & Satow, 1993).

Extinction correction by least-squares procedures is justified provided the analysis satisfies conditions on which the validity of the least-squares principle depends. Those conditions are specified by the Gauss–Markov theorem (*e.g.* Prince, 1982): the most probable parameters minimize the weighted sum-of-squares of components if their contributions to the residual are independent, and distributed normally with unit variance. Least-squares methods can be very sensitive to a few large residuals. Least-squares results may be affected significantly if large differences between the observed data and the model predictions occur more frequently than is predicted for a normal distribution. In view of this the corresponding distributions of residuals (*e.g. International Tables for Crystallography*, 1992, Vol. C) for the calcite and corundum data sets were compared. The tails of the distribution of residuals for the calcite data were smoother and more uniform than those for the corundum data sets which were much more jagged, with large residuals occurring more frequently. This may explain the different behaviour of least-squares extinction corrections for these structurally related crystals.

Table 1. *Experimental and refinement data for* $CaCO_3$

Radiation	Mo $K\alpha$
λ (Å)	0.71073
Diffractometer	Syntex *P*3
Monochromator	Graphite
Scan speed (° min $^{-1}$)	2.03
Peak scan width $[l + r + (2\theta_{K\alpha1} - 2\theta_{K\alpha2})d]$	0.9; 1.0; 1.0
Maximum 2θ (°)	100
Max. intensity variation of standards [±($\bar{1}$02), ±(0$\bar{1}$4), ±(204)] (%)	7.6
No. of observed reflections [$I > 1\sigma(I)$]	3370
Transmission range	0.841–0.887
No. of independent reflections	328
Extinction,† r^*	0.48 (3) × 10^4
Min. extinction y,‡ (hkl)	0.80, ($\bar{1}$14)
$R_{int}(F^2)$	0.033
After absorption	0.030
Extinction applied	0.029
R	0.017
wR	0.023
S	4.52
Max. shift/e.s.d.	0.00004
Extinction§ refined, r^*	0.48 (4) × 10^4
Min. extinction y,§ (hkl)	0.81, (0$\bar{1}$4)
R	0.017
wR	0.022
S	4.79
Max. shift/e.s.d.	0.00003

† Maslen & Spadaccini (1993) approach.

‡ $F_{obs} = yF_{kin}$ where F_{kin} is the value of the kinematic structure factor.

§ Zachariasen (1967) extinction corrections included in least-squares structure refinement (Larson, 1970).

Table 2. *Fractional coordinates x, anisotropic vibration parameters* U_{ij} (Å^2) *and selected interatomic distances for* $CaCO_3$ (Å)

6 Ca on 6(*b*)	U_{11}	0.01024 (8)	C—O	1.284 (1)
(0,0,0)	U_{33}	0.0098 (1)		[1.293 (3)]*
			Ca—O	2.359 (1)
6 C on 6(*a*)	U_{11}	0.0091 (3)	O—O1^i	2.224 (2)
(0,0,¼)	U_{33}	0.0106 (5)	O—O2^{ii}	3.189 (1)
			O—O3^{iii}	3.260 (2)
18 O on 18(*e*)	x	0.2573 (2)	O—O4^{iv}	3.4102 (8)
(x,0,¼)	U_{11}	0.0115 (2)		
	U_{22}	0.0222 (4)		
	U_{33}	0.0195 (4)		
	U_{13}	−0.0040 (2)		

Symmetry code: (i) $-y, x-y, z$; (ii) $\frac{2}{3}-x, \frac{1}{3}-y, \frac{1}{3}-z$; (iii) $1-y, x-y, z$; (iv) $\frac{2}{3}+y, \frac{1}{3}-x+y, \frac{1}{3}-z$.

* The C—O distance corrected for riding motion.

Structural parameters

The Ca, C and O atoms are all on special positions. The only positional parameter not constrained by

† Lists of structure factors and a figure showing a deformation-density section in the (01$\bar{1}$0) plane through the Ca, C and O atoms for the extinction parameter included in the structure refinement have been deposited with the British Library Document Supply Centre as Supplementary Publication No. SUP 55984 (5 pp.). Copies may be obtained through The Technical Editor, International Union of Crystallography, 5 Abbey Square, Chester CH1 2HU, England. [CIF reference: AS0621]

symmetry is the x coordinate for O. The refined parameters (Table 2) are within 2.5 e.s.d.'s of the values of Effenberger, Mereiter & Zemann (1981), except that the U_{11} parameters are larger, although within 5 e.s.d.'s of those reported earlier. The Ca atom in $CaCO_3$ is located at the centre of symmetry on the threefold axis, taken as the origin of unit cell (Table 2). The Ca cation coordinates with six O atoms forming an octahedron (Fig. 1) which is slightly flattened in the direction of the hexagonal c axis. Within any given layer normal to c, the octahedra are independent, sharing neither edges nor corners. Octahedra are linked *via* CO_3 groups within the layers and through their corners to the layers above and below. The C—O bonds are aligned parallel to a and the equivalent axes. Each O atom is bonded to one C and two Ca cations, each from adjacent cation layers.

Noting the relationship of the calcite and corundum structures, the O-atom geometry in calcite can be regarded as approximate hexagonal close packing, with Ca atoms at the octahedral interstices. Each O atom coordinates with only one C atom, resulting in a hexagonal distribution of C atoms in the layer of hexagonally packed O atoms. Each Ca atom fills octahedral interstices between O-atom layers that avoid coordination with two O atoms of the same CO_3 group, which is expected since the O—O1 distance is too short to occur in a near-regular coordination polyhedron (Fig. 1 and Table 2). The shortest distance between O atoms from different CO_3 groups in calcite is 3.189 (1) Å for O—O2.

All interatomic distances in Table 2 agree within 1 e.s.d. with recent refinements of calcite-type carbonates (Effenberger, Mereiter & Zemann, 1981). The C—O bond length from Table 2, although 0.003 (1) Å longer than that for calcite given in that paper, is close to the C—O bond lengths reported for other calcite-type carbonates. This difference is observed after the correction for riding motion (Table 2) evaluated by the method of Schomaker & Trueblood (1968). Rigid-body analysis of the CO_3

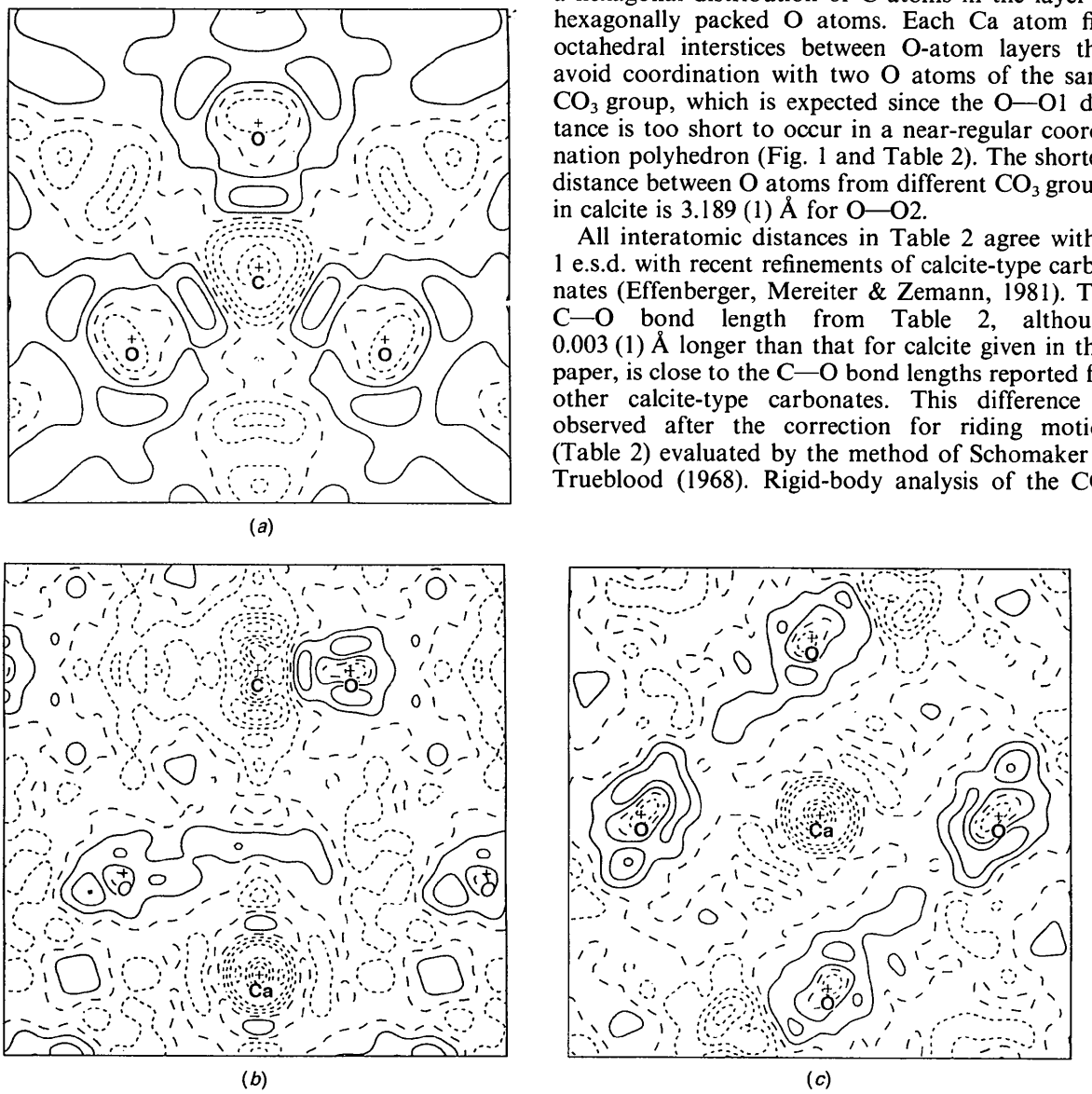

Fig. 2. $\Delta\rho$ for $CaCO_3$, evaluated with extinction corrections that minimize differences between equivalent reflection intensities. (*a*) (0001) plane through three O atoms of the CO_3 group; map borders 4.4 by 4.4 Å. (*b*) (01$\bar{1}$0) plane through Ca, C and O atoms with two O atoms deviating from the plane by 0.33 Å shown in italics; map borders 6.9 by 6.9 Å. (*c*) Equatorial plane of a CaO_6 octahedron; map borders 6.6 by 6.6 Å. Contour interval 0.1 $Å^{-3}$, positive and negative contours are depicted by solid and short dashes, respectively.

group is consistent with the weak screw motion along the *c*-axis direction, previously identified by Peterson, Ross, Gibbs, Chiari, Gupta & Tossell (1979). Attempts to improve the least-squares structural model by including disordered CO_3 groups did not show fitting improvements that were significant within the data accuracy.

The {104} cleavage plane in the calcite structure, which is common to the whole isomorphous series of minerals (Reeder, 1983), must reflect relative bond strengths in the structure. The C—O bond strength calculated by Brown & Shannon (1973) is approximately four times that of the Ca—O bond in calcite. The plane {1 0 4} in Fig. 1 breaks Ca—O bonds and no C—O bonds.

Electron density

Atomic charges determined by projecting the electron-difference density $\Delta\rho$ onto atomic density basis functions (Hirshfeld, 1977) are Ca +0.16 (2), C +0.23 (2) and O −0.13 (1) e. The relative values of these charges in calcite correspond closely to the electron-density redistribution based on atomic electronegativites, but their magnitudes are significantly less than the formal oxidation values.

Sections of $\Delta\rho$ in the (0001) plane for calcite through the C and O atoms, in the $(01\bar{1}0)$ plane through Ca, C and O, and in the equatorial plane of the Ca octahedron are shown in Figs. 2(*a*), 2(*b*) and 2(*c*), respectively. These are based on the extinction corrections determined from equivalent reflection intensities by the method of Maslen & Spadaccini (1993). The almost identical difference-density sections for the extinction parameter included in the structure refinement (Larson, 1970) are not presented here. One of these sections equivalent to Fig. 2(*b*) is to be found in the supplementary material. The 0.1 e $Å^{-3}$ contour interval is more than three times the value of $\sigma(\Delta\rho) = 0.03$ e $Å^{-3}$ evaluated by the method of Cruickshank (1949).

The general topography of these $\Delta\rho$ maps is similar to that for magnesite reported by Göttlicher & Vegas (1988). However, the maxima in the $\Delta\rho$ maps for calcite are lower (0.28 e $Å^{-3}$) than those for magnesite (0.50 e $Å^{-3}$). This can be attributed to greater exchange depletion when the more diffuse radial electron distribution of the Ca cation overlaps with the CO_3 group. Exchange terms in the wavefunction increase the effective internuclear repulsions by removing electron density from the inter-nuclear region when electrons with parallel spins overlap strongly. The cation–oxygen distances in the rhombohedral carbonates are smaller than those in the cubic oxides and are also smaller than the sums of the Goldschmidt ionic radii (Lippmann, 1973), except for magnesite.

The $\Delta\rho$ maps (Figs. 2*a* and 2*b*) do not show any obvious deviation from planarity or disorder affecting the CO_3 group. As might be expected there is excess density at the middle of each C—O bond with maximum height of 0.26 e $Å^{-3}$. A broad cloud of maximum density 0.28 e $Å^{-3}$ surrounds each O atom. Two $\Delta\rho$ peaks within that cloud, shown in Fig. 2(*a*), are within the lone-pair region. These maxima, which are elongated out of the CO_3 plane, are directed toward the Ca atoms, subtending an angle of 110° at the O atom. The Fig. 2(*b*) section shows the maxima above and under the O atom. Elongation of these maxima in the *c* direction perpendicular to the C—O bond may be a consequence of π bonding between the C and O atoms.

The density in the Ca—O bonds is depicted in Fig. 2(*c*). The $\Delta\rho$ density near the middle of each Ca—O line does not have the positive value regarded by some authors as typical of covalent interactions. This conflicts with predictions based on the earler studies for magnesite and dolomite. There is an extended region of positive density, about 0.1 e $Å^{-3}$ high, between neighbouring O atoms, 3.260 (2) Å apart, belonging to different CO_3 groups. This might be considered as reflecting weak overlap of the O-atom lone pairs in the *xy* plane, observed opposite the C—O bonds in Fig. 2(*a*), and as a diffuse cloud extending from the O atoms perpendicular to the *c* axis in Fig. 2(*b*). The significance of that overlap was suggested by Göttlicher & Vegas (1988) in $MgCO_3$. There is no similar increase in density along the longest edge of the CaO_6 octahedron, of length 3.4102 (8) Å, in Fig. 2(*c*). There is a $\Delta\rho$ maximum, 0.16 e $Å^{-3}$ high, near the midpoint of the short non-bonding contact between the O atoms, of length 3.189 (1) Å, which is not an edge of the Ca octahedron. This contact is shorter than any of the O—O edges in the CaO_6 octahedra in calcite. As mentioned above, it is the largest contact of this type in the series of rhombohedral carbonates (Effenberger, Mereiter & Zemann, 1981).

We acknowledge Dr Dudley Creagh for his calculations. This work was supported by the Australian Research Council.

References

ALCOCK, N. W. (1974). *Acta Cryst.* A**30**, 332–335.
BROWN, I. D. & SHANNON, R. D. (1973). *Acta Cryst.* A**29**, 266–282.
CREAGH, D. C. (1992). Private communication.
CRUICKSHANK, D. W. J. (1949). *Acta Cryst.* **2**, 65–82.
EFFENBERGER, H., KIRFEL, A. & WILL, G. (1983). *Tschermaks Mineral. Petrogr. Mitt.* **31**, 151–164.
EFFENBERGER, H., MEREITER, K. & ZEMANN, J. (1981). *Z. Kristallogr.* **156**, 233–243.

GÖTTLICHER, S. & VEGAS, A. (1988). *Acta Cryst.* B**44**, 362–367.
HALL, S. R., FLACK, H. D. & STEWART, J. M. (1992). *XTAL*3.2 *Reference Manual*. Univs. of Western Australia, Australia, and Maryland, USA.
HELLWEGE, K.-H. (1966). Editor. *Landoldt-Börnstein*. New Series, Group III, Vol. 1, p. 13. Berlin: Springer-Verlag.
HIRSHFELD, F. L. (1977). *Isr. J. Chem.* **16**, 198–201.
LARSON, A. C. (1970). *Crystallographic Computing*, edited by F. R. AHMED. Copenhagen: Munksgaard.
LIPPMANN, F. (1973). *Sedimentary Carbonate Minerals*. New York: Springer-Verlag.
MASLEN, E. N. & SPADACCINI, N. (1993). *Acta Cryst.* A**49**. In the press.
MASLEN, E. N., STRELTSOV, V. A., STRELTSOVA, N. R., ISHIZAWA, N. & SATOW, Y. (1993). *Acta Cryst.* B**49**. Submitted.
PETERSON, R. G., ROSS, F. K., GIBBS, G. V., CHIARI, G., GUPTA, A. & TOSSELL, J. A. (1979). *Trans. Am. Geophys. Union*, **60**, 415.
PRINCE, E. (1982). *Mathematical Techniques in Crystallography and Materials Science*. New York: Springer-Verlag.
REEDER, R. J. (1983). Editor. *Carbonates: Mineralogy and Chemistry, Reviews in Mineralogy*, Vol. 11, pp. 1–47. Chelsea, Michigan: Bookcrafters.
REES, B. (1977). *Isr. J. Chem.* **16**, 180–186.
SCHOMAKER, V. & TRUEBLOOD, K. N. (1968). *Acta Cryst.* B**24**, 63–76.
STEVENS, E. D. (1974). *Acta Cryst.* A**30**, 184–189.
STRELTSOV, V. A. & MASLEN, E. N. (1992). *Acta Cryst.* A**48**, 651–653.
STRELTSOV, V. A. & ZAVODNIK, V. E. (1989). *Sov. Phys. Crystallogr.* **34**(6), 824–828.
ZACHARIASEN, W. H. (1967). *Acta Cryst.* A**23**, 558–564.

Acta Cryst. (1993). B**49**, 641–646

Jahn–Teller Distortion of the Electron Density in α-Nickel Sulfate Hexahydrate

BY J. R. HESTER AND E. N. MASLEN

Crystallography Centre, University of Western Australia, Nedlands, Western Australia 6009, *Australia*

A. M. GLAZER

*Clarendon Laboratory, University of Oxford, Parks Road, Oxford OX*1 3*PU, England*

AND K. STADNICKA

Faculty of Chemistry, Jagiellonian University, ul. Karasia 3, 30-060 *Krakow, Poland*

(*Received* 2 *December* 1992; *accepted* 17 *February* 1993)

Abstract

The electron density at room temperature has been determined for α-nickel sulfate hexahydrate, α-$NiSO_4.6H_2O$: tetragonal, $P4_12_12$, $M_r = 262.86$, $a = 6.783$ (1), $c = 18.288$ (2) Å, $V = 841.4$ (3) Å^3, $Z = 4$, $D_x = 2.075$ Mg m^{-3}, Mo $K\alpha$, $\lambda = 0.71069$ Å, $\mu = 2.58$ mm^{-1}, $F(000) = 544$. $R = 0.023$, $wR = 0.026$ from 1864 independent reflections using X-ray diffraction data from a previous study of its structure, absolute chirality and optical activity [Stadnicka, Glazer & Koralewski (1987). *Acta Cryst.* B**43**, 319–325]. Although the charge on the $[Ni(H_2O)_6]$ moiety of 1.7 (2) e determined by partitioning the difference density is close to the formal value, the Ni atom carries a net negative charge of -0.46 (2) e. Contrary to expectation, only four lobes of electron density are evident in the vicinity of the Ni atom. They are aligned toward the four second nearest-neighbour S atoms. Along the Ni—S vectors the maximum $\Delta\rho$ is 1.3 e Å^{-3}. There is no significant concentration of the electron density in other directions.

Introduction

The structure consists of S—Ni layers normal to the c axis (Fig. 1). The S—Ni—S angles are 90°. Each Ni atom is coordinated to six water molecules in an octahedral configuration with each hexaaquanickel moiety linked *via* a hydrogen-bond network to the four coplanar sulfate groups shown in Fig. 2(*a*). These groups lie 4.8 Å from the Ni atom and two lie along a twofold axis in the [110] direction. The hexaaquanickel moiety is also connected by the hydrogen-bond network to two sulfate groups in the layers above and below the Ni atom (Fig. 3*a*). These sulfate groups are located 5.4 Å from the Ni. Because the geometries of the first and second nearest-neighbour interactions are distinctly different, this structure provides a means of assessing their relative importance.